Bulletin of Earth Sciences of Thailand

APPLICATION OF POST-STACK SEISMIC INVERSION AND ITS LIMITATIONS FOR MAPPING OF FLUVIAL SYSTEMS IN WESTERN PATTANI BASIN, GULF OF THAILAND

Phanat Thatmali*

Department of Geology, Faculty of Science, Chulalongkorn University, Bangkok, 10330, Thailand
*Corresponding author e-mail: p-thatmali2011@hotmail.com

Abstract

Reservoir rocks in the Pattani Basin are fluvial sandstones which are highly compartmentalized due to their complex depositional and structural evolution. Imaging of these reservoirs is not always possible using conventional seismic data. This study presents rock physics analysis for the feasibility of post-stack seismic inversion within different sequences of the western part of the Pattani Basin. The post-stack seismic inversion was executed for the mapping of fluvial reservoir sands. Rock-physics results reveal that P-impedance values of sands are less than shales in the late Middle Miocene and Early Miocene depositional sequences. Some of the thin shales within the early Middle Miocene have very low P-impedance that is equivalent to sands. These are interpreted as marginal marine coaly mudstones. Blind tests demonstrated that sands could be differentiated from shales in Early Miocene and partially differentiated in the late Middle Miocene sequences. Geomorphological analysis of horizon slices extracted from P-impedance volumes showed that sands associated with the channels are narrow and of high sinuosity in the Early Miocene and early Middle Miocene, whereas wide channels were observed in the late Middle Miocene. Marine influence has been inferred from the presence of marginal marine coaly mudstone. The marine incursions are more dominant in early Middle Miocene sequence and initiated in Early Miocene from the southeastern part of the area.

Keywords: P-impedance, post-stack seismic inversion, marginal marine coaly mudstone, Pattani basin

1. Introduction

The Gulf of Thailand is comprised of a number of north-south oriented rift basins. The reservoirs in these basins are sands associated with fluvial systems. They have complex geometries due to their depositional style combined with intense compartmentalization created by faults related to the structural evolution of the basins. Due to these structural and stratigraphic complexities, it is common to encounter different sand facies with various fluid content. Therefore, it is important to develop an optimal geophysical workflow to image the reservoirs of the area.

Rock physics analysis and post-stack seismic inversion technique were applied on seismic data of Dara field in the western part of the Pattani Basin. There have been a few attempts to predict sand distribution by using the seismic attributes and seismic inversion (Ahmad and Rowell, 2012, and Ahmad and Rowell, 2013) in the central part of the Pattani Basin. However, no study has been reported for the western area of the Pattani Basin. Moreover, previous studies analyzed different rock physics parameters as a function of depth and concluded that post-stack seismic inversion is not effective beyond a certain depth. In this study, I analyzed various rock physics parameters with respect to different stratigraphic intervals and attempted to explore the rock properties of various lithologies in each depositional sequence. The key objectives of the present study are;

1. To conduct rock physics analysis to determine lithology and fluid sensitive rock properties in each stratigraphic sequence.
2. To evaluate the feasibility of post-stack seismic inversion technique for lithology and hydrocarbon discrimination.
3. To map fluvial sands and generate a depositional model by integrating seismic inversion and well log data.

2. Study area

The study area is in western part of Pattani basin. The Pattani basin is the largest of a series of elongated N-S trending Tertiary rifts formed in the Gulf of Thailand (Figure 1). It is a result

of crustal extension caused by the Indianplate northward movement and collided into the Eurasia plate during the Tertiary. The structural style in Pattani Basin is dominant by Eocene to Oligocene syn-rift sequence that is buried by deep (6-8km) and followed by very rapidly subsiding Miocene-Recent post-rift event (Morley et al, 2011).

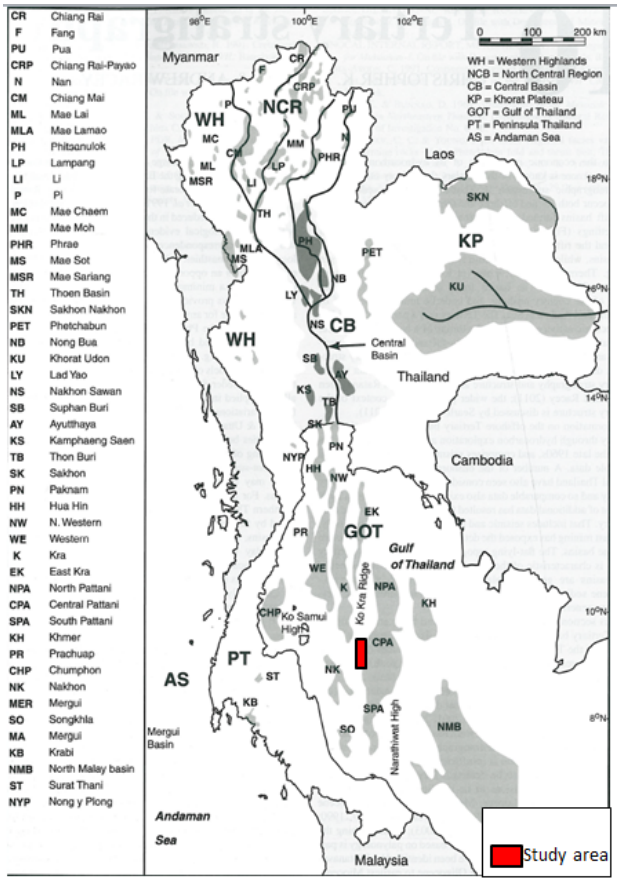

Figure 1. Location map of study area within Pattani basin, Gulf of Thailand (modified from Morley and Racey, 2011)

The stratigraphy in this area can be subdivided into 5 sequences (e.g. Jardine, 1997; Morley and Racey, 2011). Sequence I began with initial localized lacustrine and alluvial deposition in the Late Eocene to Oligocene. The top of this sequence was marked by Mid- Tertiary Unconformity (MTU) around 25 Ma, then mostly fluvial and alluvial deposited in the Early Miocene of Sequence II. After that, transgressive fluvial and /deltaic with some marginal marine deposits in the early Middle Miocene of Sequence III, then overall regressive fluvial and alluvial deposition in the late Middle Miocene of Sequence IV. The top of Sequence IV was marked by Middle Miocene unconformity (MMU) around 10 Ma, and predominately transgressive marginal marine deposition in the Late Miocene of Sequence V.

As regional depositional environments vary from fluvial to marginal marine, Three different types of organic-rich sediments were identified by Kamvan (2013), Champasa (2015), and Narapan (2015). They are comprised of marginal marine shale which has low resistivity and moderate-high density, marginal marine coaly mudstone which has high gamma ray and spiky density and neutron curves and non-marine coaly mudstone which with low density and low GR values. These organic-rich sediments are dominant within Sequence III.

3. Methodology

3.1 Rock physics

The main purpose of rock physics is to determine rock properties to differentiate lithology and reservoir fluids. The key purpose of rock physics in this study to evaluate the feasibility of post-stack seismic inversion for reservoir characterization. Cross-plots of P-impedance versus shale volume color coded by water saturation and porosity for different stratigraphic intervals within the reservoir zone were analyzed. This study also used P-impedance versus depth cross-plot to analyze the depth influence on various rocks properties. The sands were identified by using shale volume less than 30% or GR value less than 90-110 API for the wells that do not have computed shale volume curve. The water saturation cutoff was set at 65% for hydrocarbon bearing sands.

3.2 Post-stack seismic inversion

Wavelet extraction is the first process for computed seismic inversion. the seismic data volume in this study was inverted into acoustic impedance volume by the model-based inversion technique. The initial model was built by supplying the missing low frequencies from the seismic by using well logs. Five horizons (near top Sequence IV called B, near top Sequence

III, called F, near top Sequence II called K, near the middle of Sequence II called O and base of inversion called Base) were used structurally to guide the interpolation of P-impedance within the initial model. After that, the model and seismic were combined to create the seismic inversion volume. Then, the original log and inverted P-impedance data were compared, and a blind test also was performed to QC the inverted volume. Horizon slices from post-stack seismic inversion volume were used to analyze sand distribution in the study area.

4. Results and discussions

4.1 Rock physics

The cross-plots analysis reveals that clean sands with GR less than 110API show low P-impedance. P-impedance increases as gamma ray increase till 150 API but P-impedance decreases for the pure shales. Clean sands can be separated by using P-impedance within the Sequence IV (below 6500 (m/s)*(g/cc)). Moreover, Gas sands have very low P-impedance (less than 5400 (m/s)*(g/cc)) (Figure 2A) but in Figure 3A which represents a well only 1.9 km away from the well shown in Figure 2A, gas sands show overlapping P-impedance with wet sands and even sands also show overlapping P-impedance with shales (Figure 3A). Therefore, P-impedance is not always useful to differentiate sands and shales and to identify hydrocarbon zones within the Sequence IV. Clean sands can be isolated by using P-impedance (below 7000 (m/s)*(g/cc)) within the Sequence III. There are some very thin shales within the Sequence III which have very low density and P-wave velocity. The P-impedance of these shales is sometimes less than gas sands. Li et al., 2014 studied a rock physics model for the characterization of organic shale. They explained that when the kerogen content increases, the velocity and density of shales decrease. Kamvan, 2013, Narapan, 2015 and Champasa, 2015 have reported marginal marine coaly mudstone with low density and P- wave velocity within the central and southern Pattani Basin, Gulf of Thailand. Therefore, the very low P-impedance shales were interpreted as marginal marine coaly mudstones in this study (Figure 2B). Clean sands can be separated by using P-impedance (below 8100 (m/s)*(g/cc)) within the Upper Sequence II. There are only a few occurrences of marginal marine coaly mudstone that show very low P-Impedance values in the range the sands. Therefore, P-impedance can be used to identify the sand within the Upper Sequence II. (Figure 2C). Clean sands can be separated by using P-impedance (less than 9300 (m/s)*(g/cc)) within the Lower Sequence II (Figure 2D). P-impedance cannot be used to identify hydrocarbon zones in all sequences.

The cross-plot of density, P-wave velocity and gamma ray color coded by water saturation reveal that the density increases as depth increases. However, sands have a lower density than shales. Only marginal marine coaly mudstones have equal or lower than density of the sands. P-wave velocity of the clean sands and the pure shales are in the same range.

The cross-plot of P-impedance and shale volume color coded by total porosity reveals that the P-impedance can indicate the high porous sand zones. The high porosity sands have relatively low P-impedance. (Figure 4)

P-impedance plot with respect to depth shows that sands have lower P-impedance than shales in the lower part of the Sequence II. Whereas in Sequence III, and the upper part of Sequence II, which are dominant by marginal marine coaly mudstone. P-impedance of shales and sands are significantly overlapping (Figure 5).

In summary, the cross-plot analysis shows that P-impedance can differentiate sand and shale within the Sequence II. Whereas it can only partially separate lithologies within the other stratigraphic sequences. P-impedance can differentiate gas sands and wet sands at some wells within the Sequence IV. The rock physics analysis reveals that rock properties of different lithologies of the area are complex and vary spatially and vertically. Therefore, application of any inversion techniques should be considered carefully for the prediction of lithologies

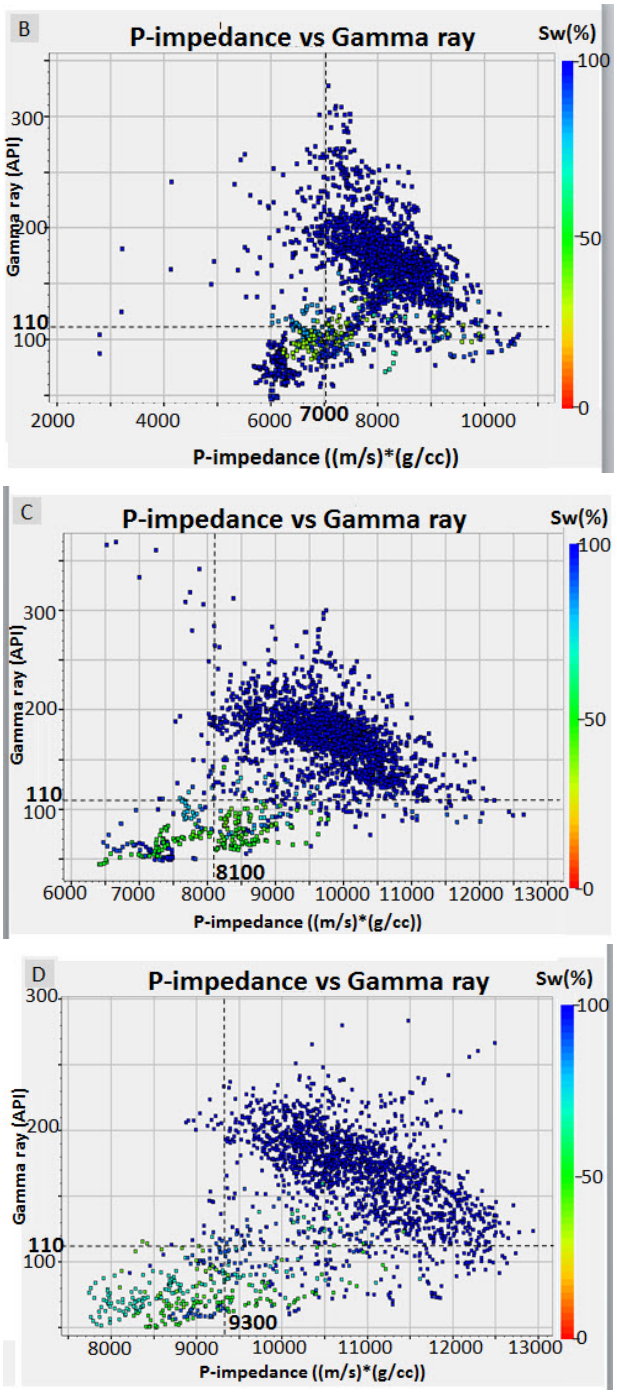

Figure 2. Cross-plot of P-impedance and gamma ray colored by water saturation for (A) Sequence IV (B) Sequence III (C) Upper Sequence II and (D) Lower Sequence II.

and hydrocarbon.

4.2 Post-stack seismic inversion

The wavelet was extracted by using 31 wells in the study area for well tie to seismic and seismic inversion process. The dominant frequency is at 18 Hz.

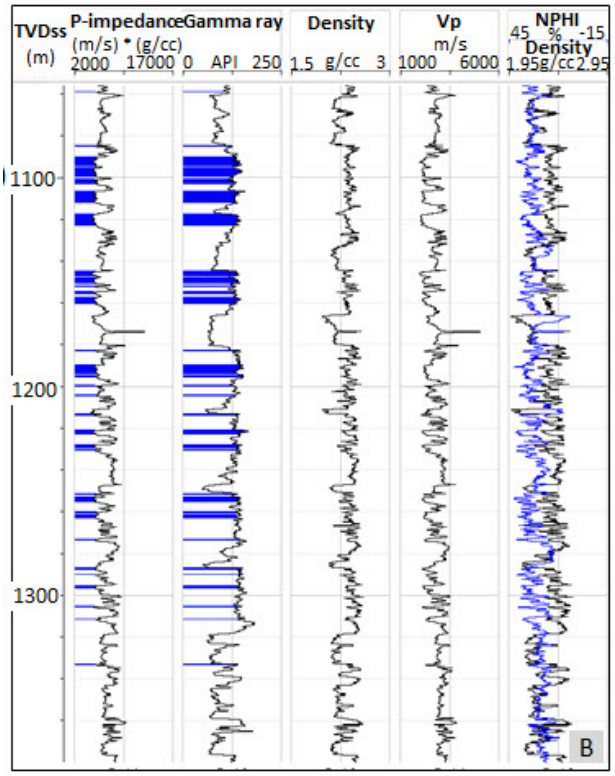

Figure 3. Cross-plot of P-impedance and gamma ray colored by water saturation for Sequence IV, highlighted area in blue (A) shown on wire line section of DA04 well (B).

The initial model was generated by using low-frequency filter at 10/15 Hz high cut frequency was used to supply the missing low frequencies in the seismic data. Eight wells were used to interpolate P-impedance throughout the area. The data was structurally interpolated by using 5 interpolated horizons (B, F, K, O, and base).

Inversion analysis of selected parameters

Before executing inversion process, the inversion analysis was performed to check the accuracy of the selected parameters. The error from a difference between the synthetic traces calculated from this inversion result compared with seismic input traces range between 354-885 and correlation of P-impedance between original log and inverted log is 0.890.

QC of Seismic Inverted Volume

The P-impedance log shows a reasonable

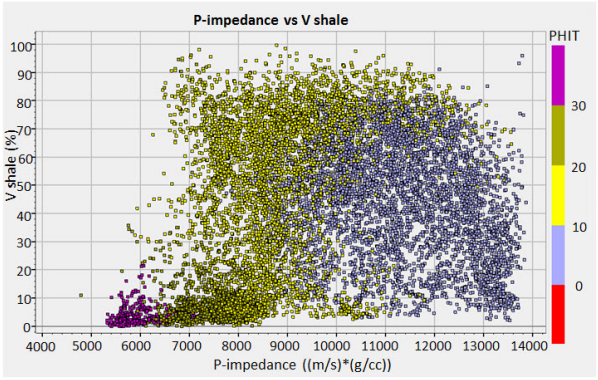

Figure 4. Cross-plot of P-impedance and shale volume colored code by total porosity

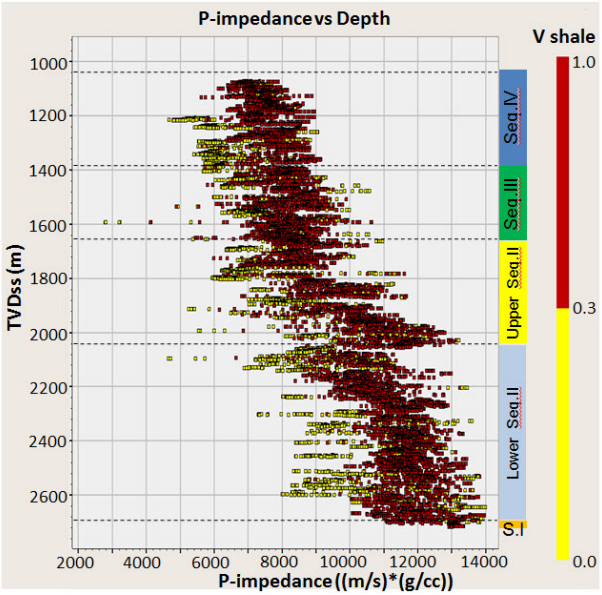

Figure 5. Cross plot P-impedance and Depth. It shows sand and shale can clearly separate in Sequence II.

match with the Inverted P-impedance volume in Sequence IV (Figure 6A) and sands are represented by low P-impedance while P-impedance log in Sequence III does not show a good match. Sands show low P-impedance, but there are some shales which also show low P-impedance. It was expected as revealed by the rock physics analysis because thin marginal marine coaly mudstones with low P-impedance were encountered in the Sequence III. The P-impedance of these shales is in the range of P-impedance of sands. Therefore, P-impedance cannot effectively differentiate lithologies within the Sequence III (Figure 6B). Excellent match between P-impedance log and P-impedance inverted volume in the Upper Sequence II (Figure 6C) and Lower Sequence II (Figure 6D).

Blind test

The blind test was performed by using wells which were not included in the inversion process to check the accuracy of the inversion. The well DAWA-20 was used for the blind test. The P-impedance values show a reasonable match with GR log. Low gamma ray responds to relative low P-impedance on inverted volume. Sands show low P-impedance. The comparison shows good match within Sequence II (Figure 7C, and 7D), and in Sequence IV (Figure 7A), In Sequence III, low P-impedance does not always represent sands as shown by a marked circle in Figure 7B. These value of low P-impedance are due to marginal marine coaly mudstone.

Sand distribution

Based on the rock physics, the cutoff for P-impedance value of sands at 6500 m/s* g/cc, 7000 m/s * g/cc, 8100 m/s * g/cc, and 9300 m/s * g/cc in Sequence IV, III, the Upper Sequence II and the Lower Sequence II respectively were defined.

Figure 8, and 9A-C show map view of P-impedance images along horizon slice with line-drawing interpretations of the meaningful geological patterns of sand distributions in each sequence. Figure 8 is the P-impedance map of horizon slice along F horizon shifted 210 ms upward in Sequence IV which shows sands are very wide and of less sinuosity, the sands are oriented almost north-south direction. Figure 9A is P-impedance map of horizon slice along F horizon shifted 57ms downward in Sequence III reveals sands are narrower and oriented in NE-SW and NW-SE direction. P-impedance map of horizon slice of K horizon shifted 20ms downward in the Upper Sequence II reveals sands are of high sinuosity and narrow as shown in Figure 9B. Figure 9C is P-impedance map of horizon slice of base horizon shifted 23 ms upward represents the sands which are narrow and have high sinuosity. These sands are oriented NS and NW-SE.

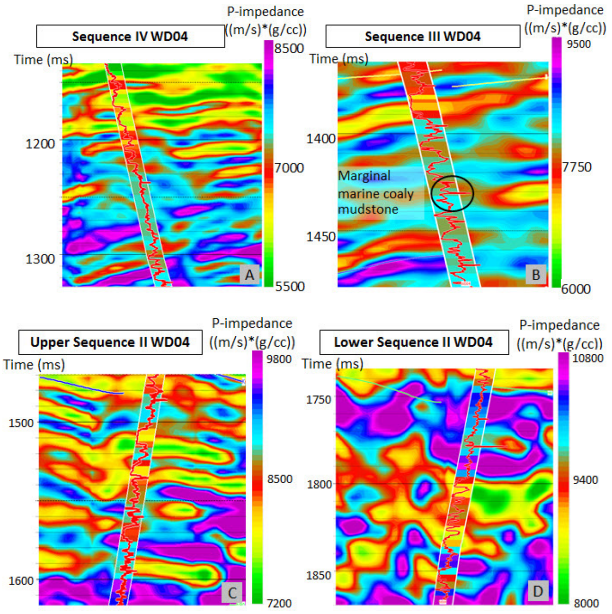

Figure 6. P-impedance volume section along WD04 well. Gamma ray and P-impedance logs are displayed for comparison the inverted volume in (A) Sequence IV, (B) Sequence III, (C) Upper Sequence II, and (D) Lower Sequence II.

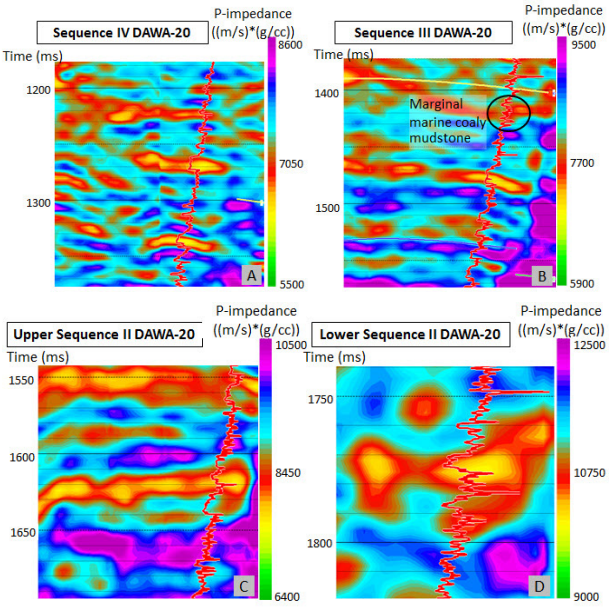

Figure 7. Blind test of DAWA-20 shows on the P-impedance section with Gamma ray log in (A) Sequence IV, (B) Sequence III, (C) Upper Sequence II, and (D) Lower Sequence II.

Marginal marine coaly mudstone distribution

The rock physics results show that there are some shales which have very low P-impedance. These shales are interpreted as marginal marine coaly mudstone. The cumulative

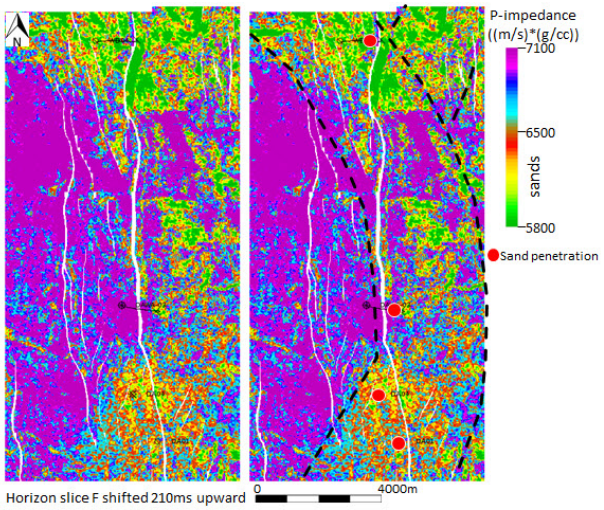

Figure 8. Sand distribution along horizon slice of P-impedance volume for Sequence IV.

thicknesses of marginal marine coaly mudstone were computed in each stratigraphic sequence (Figure 10) to observe the lateral distribution these sediments. The marginal marine coaly mudstones occurred very rarely in Sequence IV and lower part of Sequence II. The maximum thickness is about 1.4 meters and 7.7 meters in Sequence IV and Lower Sequence II respectively. However, these shales are abundant within the Sequence III and upper part of Sequence II. The maximum total accumulative thicknesses in Sequence III and Upper Sequence II are 21.6 and 29.8 meters respectively. These marginal marine coaly mudstones are thickest within the graben structure for Sequence III (Figure 10A).

The marginal marine coaly mudstones indicate marine influence in the study area. The marine influence initiated from the southeastern part of the Lower Sequence II and the thickness of these sediments is more in the southeastern part of the area in Sequence II and Sequence III shows the thickest portion of these shales within the graben structure. Sequence IV does not have a significant thickness of these organic-rich sediments (Figure 10 D-F).

Depositional environment

Paleoenvironments were inferred based on marginal marine coaly mudstone cumulative thickness maps and seismic geomorphology

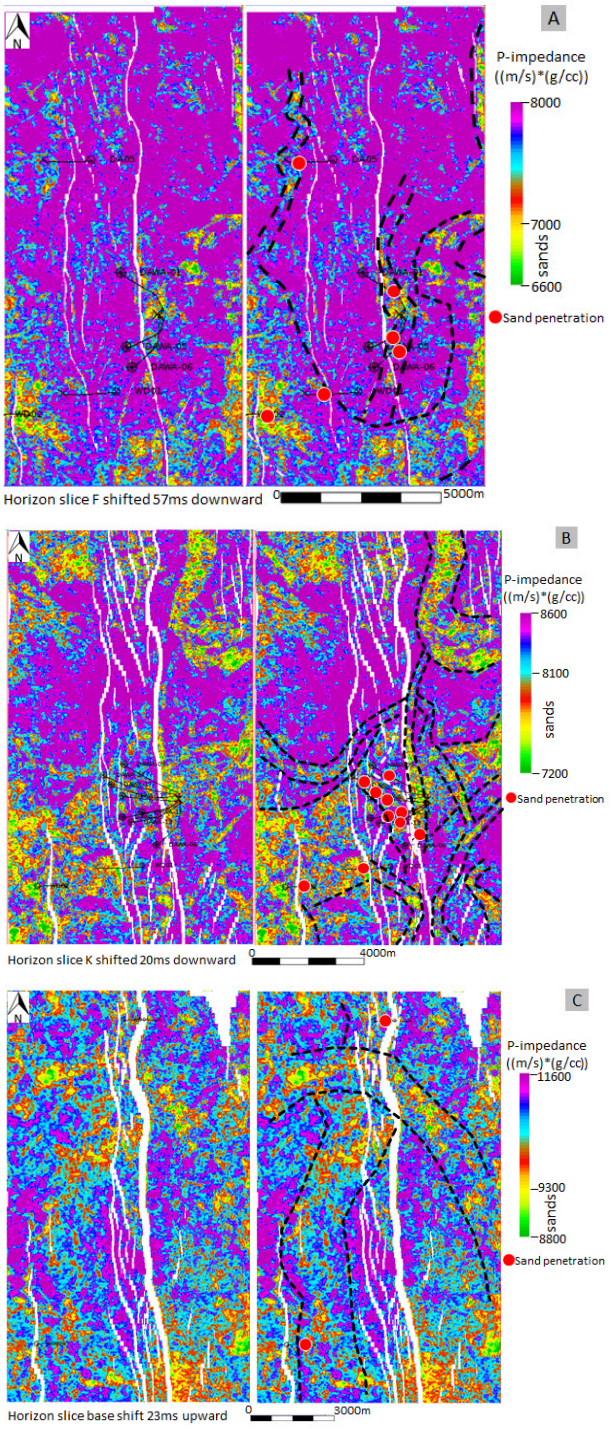

Figure 9. Sand distribution along horizon slice of P-impedance volume (A) Sequence III (B) Upper Sequence II, and (C) Lower Sequence II.

observed on horizon slices. The early Early Miocene interval has predominantly alluvial plain deposit. Occasional occurrences of marginal marine elements in the southeastern part indicate marine influence. The late Early Miocene to early Middle Miocene was dominant by marginal marine coaly mudstones indicating marine influence in this interval. The wells located in the graben structure and eastern part of study area have a higher degree of marine influence, demonstrating that the marine incursion came from the southeast. The horizon slices within these intervals show narrow channels are sands are not abundant within these intervals. The late Middle Miocene was dominant by fresh water and lack of marine influence (Figure 11). This interval shows well developed broader fluvial meander belts.

5. Conclusions

Rock physics analysis and model based post-stack seismic inversion were applied to characterize the Miocene reservoir sands in the western part of the Pattani Basin. Key findings and conclusions are summarized below.

- P-impedance depends upon depth and lithology. The clean sands have low P-impedance, and it increases as shale content increases until 40% shale volume. Beyond 40% shale volume, P-impedance start decreases.
- P-impedance can successfully differentiate sands and shales in Sequence II (Early Miocene) and partially differentiate lithologies in Sequence IV (late Middle Miocene) and Sequence III (early Middle Miocene). The overlap of P-impedance for these two lithologies is more intense in Sequence III (early Middle Miocene) as compared to other sequences because Sequence III has marginal marine coaly mudstones, which show very low P-impedance.
- Post-Stack seismic inversion solving for P-impedance volume may not be useful for identification of hydrocarbon zones as water-bearing sands and hydrocarbon bearing sands show P-impedance in the same range.
- P-impedance volume can provide information about the porosity as high porosity zones shows low P-impedance.

meander belts.

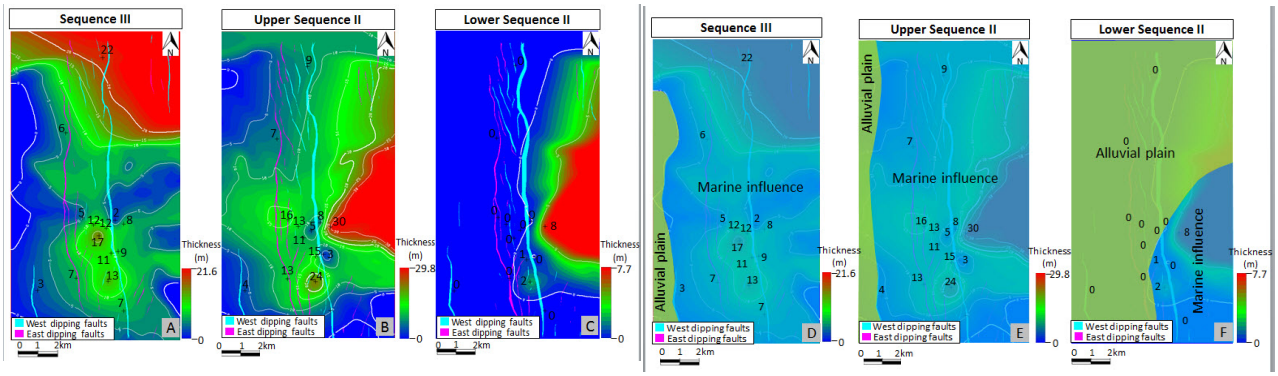

Figure 10. Marginal marine coaly mudstone cumulative thickness map (A) Sequence III, (B) Upper Sequence II, (C) Lower Sequence II. Interpreted map of depositional environment over marginal marine coaly mudstone cumulative thickness map (D) Sequence III, (E) Upper Sequence II, (F) Lower Sequence II. These can be indicate marine ame from the southeastern part of study area.

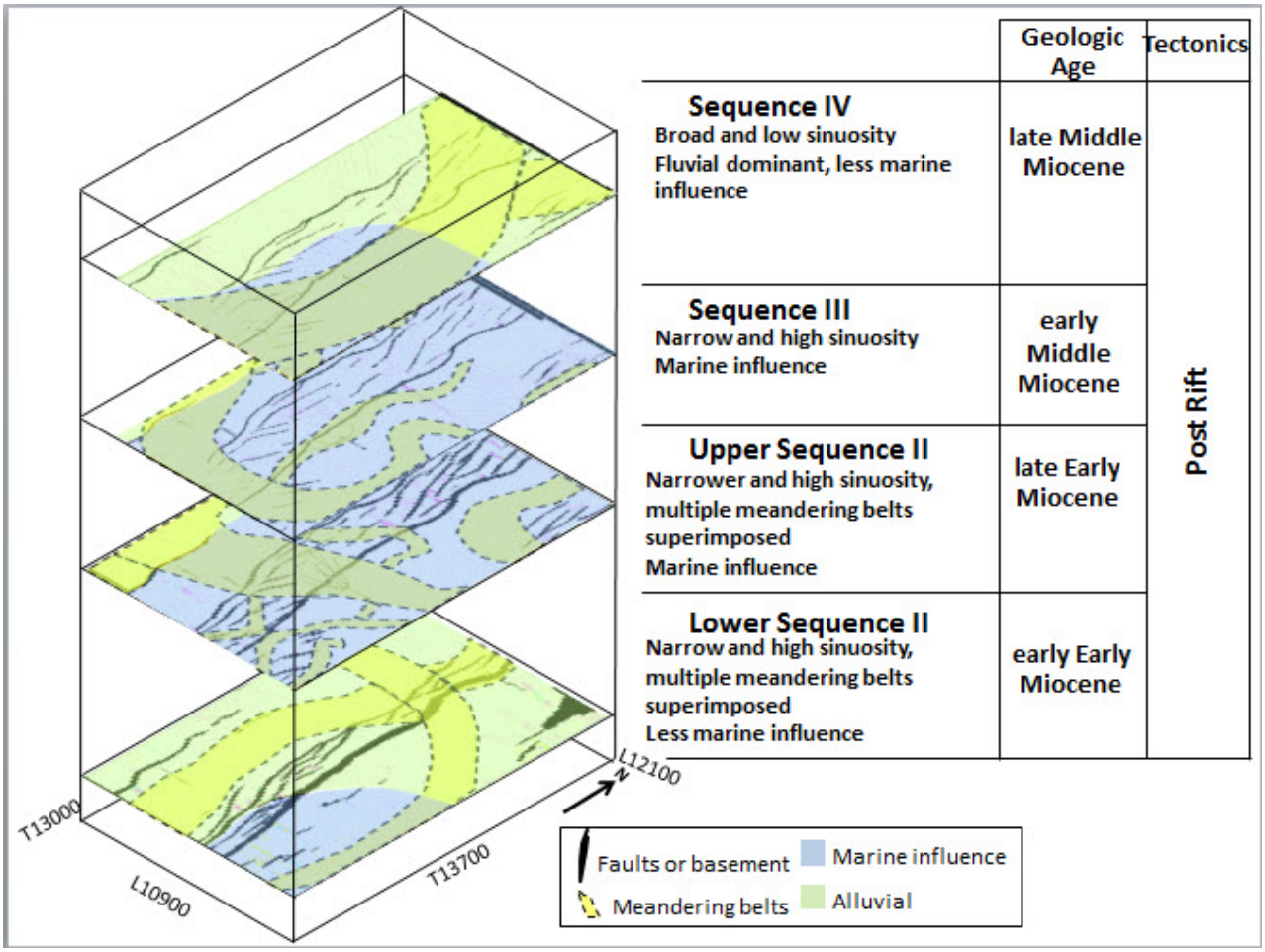

Figure 11. Deposition Model within the study interval.

- P-impedance volume can provide information about the porosity as high porosity zones shows low P-impedance.
- The blind test indicated a reasonable match of inverted seismic volumes and well data. Post-stack seismic inversion was successful for the prediction of the sands in Lower Sequence II (early Early Miocene) and partially successful in Sequence IV (late Middle Miocene)

and Upper Sequence II (late Early Miocene). However, it is very difficult to separate sand and shale based on P-impedance within the Sequence III (early Middle Miocene) due to the presence of low P-impedance marginal marine coaly mudstone.

- Sequence III (early Middle Miocene) is mostly influenced by marine incursions as marginal marine mudstones are abundant within this sequence. The marine incursions started from the southeastern part of the area in the Lower Sequence II (early Early Miocene).
- Rock physics properties of different lithologies are complex and vary spatially and vertically. Therefore, the application of any seismic inversion technique should be considered carefully for the prediction of lithology and hydrocarbon prediction.

6. Acknowledgement

I would like to express my deepest gratitude to my supervisor Dr. Mirza Naseer Ahmad for his excellent guidance, patience, and caring for doing my research. I am truly thankful to Chevron Thailand Exploration and Production, Ltd. For providing scholarship and the data for this study. Finally, I gratefully acknowledge my parents and my friends for all their support throughout the year.

7. References

Application of Spectral Decomposition and SeismicAttributes to Understand the Structure and Distribution of Sand Reservoirs within Tertiary Rift Basins of Gulf of Thailand: The Leading Edge, v.31, no.6, p.630-634.

Ahmad, M.N., and P. Rowell, 2013, Mapping of fluvial sand sytems using rock physics analysis and simultaneous inversion for density: case study from the Gulf of Thailand: First break, v.31, p.49-54.

Champasa, P.,2015, Different Types of Organic-Rich Geological Markers in Surat, Central North of Pattani Basin, Gulf of Thailand, Master's thesis, Chulalongkorn University, Bangkok, Thailand, 42 p.

Jardine, E., 1997, Dual petroleum systems governing the prolific Pattani basin, offshore Thailand: Indonesian Petroleum Association Proceedings of the Petroleum Systems of SE Asia and Australia Conference, p. 351-355.

Kamvan, J.,2013, The Different Types of Organic-Rich Geological Markers in the Sub-Surface in the North Pailin Field, Pattani Basin, Gulf of Thailand, Master's thesis, Chulalongkorn University, Bangkok, Thailand, 52p.

Li, Y., Z.Q. Guo, C. Liu, X. Y. Li, and G. Wang, 2015, A rock physics model for the characterization of organic-rich shale from elastic properties: Petroleum Science, v.12, no. 2, p.264-272

Morley, C.K., P. Charusiri, and I.M. Watkinson, 2011, Structural geology of Thailand during the Cenozoic, in Ridd, M.F., A.J.Barber, and M.J.Crow, eds., The Geology of Thailand: London, Geological Society, p.273-334

Narapan, J.,2015, Different Types of Organic-Rich Geological Markers in South Pailin Field, Pattani Basin, Gulf of Thailand, Master's thesis, Chulalongkorn University, Bangkok, Thailand, 51 p.